Suppression of Activation and Induction of Apoptosis in RAW264.7 Cells by Amniotic Membrane Extract

Hua He,[1] *Wei Li,*[1,2] *Szu-Yu Chen,*[1] *Shan Zhang,*[1] *Ying-Ting Chen,*[1] *Yasutaka Hayashida,*[1] *Ying-Ting Zhu,*[1] *and Scheffer C. G. Tseng*[1]

Purpose. Macrophages play a pivotal role in initiating, maintaining, and resolving host inflammatory/immune responses but may cause recalcitrant inflammation and tissue damage if not controlled. Clinically, amniotic membrane (AM) transplantation suppresses inflammation in ocular surface reconstruction. Experimentally, the authors and others have reported that AM facilitates macrophage apoptosis. However, it remains unclear whether such anti-inflammatory activity is retained in AM extract (AME).

Methods. Herein the authors demonstrate in resting and activated (by interferon [IFN]-γ, lipopolysaccharide [LPS], or IFN-γ/LPS) murine monocyte/macrophage RAW264.7 cells that AME suppresses cell spreading and reduces actin filaments determined by phalloidin staining and Western blotting of Triton X-100 extracted cell lysate.

Results. Western blot and immunocytochemistry staining showed AME downregulates the expression of such cell surface markers as CD80, CD86, and major histocompatibility complex class 2 antigen. Cell growth/viability is inhibited whereas cell apoptosis is enhanced by AME. Accordingly, secreted proinflammatory cytokines such as TNF-α and IL-6 are reduced, but anti-inflammatory cytokine IL-10 is upregulated.

Conclusions. Collectively, these results suggest that, similar to amniotic membrane, AME retains anti-inflammatory activities and does so by downregulating activation and inducing apoptosis in macrophages. (*Invest Ophthalmol Vis Sci.* 2008; 49:4468–4475) DOI:10.1167/iovs.08-1781

Inflammation is a common host immune response to diseases or tissue injury; however, prolonged inflammation is detrimental to the host. Macrophages play a pivotal role in initiating, maintaining, and resolving host inflammatory responses (for a review, see Singer and Clark[1]) by killing viruses, bacteria, and parasites and acting as scavenger cells. On the other hand, macrophages also exert deleterious effects on the host by inducing proinflammatory cytokines. These deleterious effects aggravate tissue damage and are responsible for many pathologic conditions associated with acute and chronic inflammation (for a review, see Duffield[2]).

Macrophages must be activated so that they can perform their specialized activities, among them killing intracellular pathogens and secreting proinflammatory mediators. Typically, macrophages are activated in vitro by exposure to two classical stimuli, interferon (IFN)-γ and lipopolysaccharide (LPS). Morphologically, activated macrophages spread out more and contain more filamentous actins than resting cells.[3] Phenotypically, activated macrophages upregulate the expression of surface molecules such as CD80 (B-7.1), CD86 (B-7.2), and major histocompatibility complex (MHC) class 2 antigen. These activated macrophages also secrete proinflammatory cytokines such as TNF-α, IL-6, and IL-12. However, activities of these activated cells must be carefully regulated to prevent uncontrolled inflammation. One mechanism involves such immunoregulatory cytokines as transforming growth factor (TGF)-β and IL-10, from macrophages or surrounding cells, to downregulate macrophage activation. Another mechanism involves facilitation of macrophage death by apoptosis to remove them.

Clinically, one novel method of reducing macrophage-mediated inflammation is to apply cryopreserved amniotic membrane (AM) to surgical or injury sites (for reviews, see Tseng and Tsubota,[4] Dua et al.,[5] and Bouchard and John[6]). AM is the innermost layer of the placental membrane; it consists of a simple epithelium, a thick basement membrane, and a subjacent avascular stroma. Experimentally, application of human AM as a temporary graft for 2 days induces rapid regression of corneal stromal edema and inflammation and reduces the infiltration of lymphocytes and macrophages in the corneal stroma in a murine model of HSV-1 necrotizing keratitis.[7] Application of human AM as a temporary graft for 24 hours also reduces the infiltration of polymorphonuclear leukocytes (PMN) in the excimer-ablated rabbit stroma while promoting apoptosis of PMNs adherent to AM stroma.[8,9] Clinically, application of AM either as a temporary graft for treating persistent corneal epithelial defects or in conjunction with keratolimbal allograft traps monocytes and macrophages and induces apoptosis.[10] These results help explain why AM suppresses inflammation when used as a temporary or permanent graft for ocular surface reconstruction (for reviews, see Tseng and Tsubota,[4] Dua et al.,[5] and Bouchard and John[6]). Recently, we reported that AM stromal matrix exerts the aforementioned anti-inflammatory actions by inducing apoptosis of IFN-γ–activated monocyte/macrophage RAW264.7 cells and that such apoptosis is not caused by nitric oxide (NO) but instead by the downregulation of antiapoptotic NF-κB and Akt-FKHR signaling pathways.[11] Herein, we demonstrated that such an anti-inflammatory activity was retained in soluble amniotic membrane extract (AME), which altered cell morphology by reducing

From [1]TissueTech, Inc. and the Ocular Surface Center, Miami, Florida.

[2]Present affiliation: Eye Institute and Xiamen Eye Center, Xiamen University School of Medicine, Fujian, China.

Supported in part by National Institutes of Health, National Eye Institute Grant R43 EY017497 (SCGT), a research grant from TissueTech, Inc., and an unrestricted grant from Ocular Surface Research and Education Foundation, Miami, Florida. The content is solely the responsibility of the authors and does not necessarily represent the official views of the National Institutes of Health.

Submitted for publication January 23, 2008; revised March 19 and April 25, 2008; accepted August 20, 2008.

Disclosure: **H. He**, Tissue Tech, Inc. (F, E); **W. Li**, Tissue Tech, Inc. (F, E); **S.-Y. Chen**, Tissue Tech, Inc. (F, E); **S. Zhang**, Tissue Tech, Inc. (F, E); **Y.-T. Chen**, Tissue Tech, Inc. (F, E); **Y. Hayashida**, Tissue Tech, Inc. (F, E); **Y.-T. Zhu**, Tissue Tech, Inc. (F, E); **S.C.G. Tseng** Tissue Tech, Inc. (F, I, E, P)

The publication costs of this article were defrayed in part by page charge payment. This article must therefore be marked "*advertisement*" in accordance with 18 U.S.C. §1734 solely to indicate this fact.

Corresponding author: Scheffer C. G. Tseng, Ocular Surface Center, 7000 SW 97 Avenue, Suite 213, Miami, FL 33173; stseng@ocularsurface.com.

Investigative Ophthalmology & Visual Science, October 2008, Vol. 49, No. 10

actin filaments, suppressed activation, and promoted cell apoptosis in resting, IFN-γ, LPS, and IFN-γ/LPS–activated monocyte/macrophage RAW264.7 cells. Secreted proinflammatory cytokines such as TNF-α and IL-6 were reduced, but anti-inflammatory cytokine IL-10 was upregulated. The significance of these findings is further discussed.

Materials and Methods

RAW264.7 cell, a mouse monocyte/macrophage cell line, was purchased from American Type Culture Collection (ATCC; Manassas, VA). Dulbecco modified eagle medium (DMEM), fetal bovine serum (FBS), phosphate-buffered saline (PBS), amphotericin B, gentamicin and 0.25% trypsin/EDTA were from Invitrogen (Carlsbad, CA). IFN-γ, LPS, BSA, Triton X-100, paraformaldehyde, Hoechst 33342, protease inhibitor cocktail, mouse monoclonal antibody to β-actin, and rabbit anti-rat IgG peroxidase-conjugated antibodies were from Sigma Chemical (St. Louis, MO). Sodium fluoride and sodium vanadate were from Fisher Scientific (Pittsburgh, PA). Plastic culture dishes were from Becton Dickinson (Lincoln Park, NJ). Antibodies to histone H3 were from Cell Signaling Technology (Beverly, MA). Fluorescein phalloidin was from Molecular Probes (Eugene, OR). Nitrocellulose membrane and 4% to 15% polyacrylamide gradient gels were from Bio-Rad Laboratories (Hercules, CA). Enhanced chemiluminescence reagent was from PerkinElmer Life Sciences (Rockford, IL). Peroxidase-conjugated antibodies of rabbit anti–mouse or goat IgG and swine anti–rabbit IgG were from DAKO (Carpinteria, CA). Immunoassays of mouse TNF-α, IL-6, and IL-10 and antibodies specific against CD80 (B7.1), CD86 (B7.2) were from R&D Systems (Minneapolis, MN). Monoclonal antibodies anti–mouse I-A^d (MHC class 2 antigen) was from BD Biosciences (Franklin Lakes, NJ). Kits for cell proliferation and ELISA were from Roche Applied Science (MTT Cell Proliferation and Cell Death Detection and ELISA^{PLUS}; Indianapolis, IN).

Preparation of AME

The preparation of human AME was carried out aseptically so that it could be used for subsequent cell cultures. The entire frozen human AM containing fetal and placental portions was obtained from BioTissue, Inc. (Miami, FL), sliced into small pieces, frozen in the liquid nitrogen, and grounded to a fine powder (BioPulverizer; Biospec Products, Inc., Bartlesville, OK). The powder was weighed and mixed with cold PBS buffer at 1:1 of weight (g)/volume (mL). The mixture was kept in the ice and homogenized with pestle/mortar (Weaton, Inc., Dremel, WI) up and down for 10 times. The homogenate was mixed for 1 hour at 4°C and was followed by centrifugation at 48,000*g* for 30 minutes at 4°C. The supernatant was designated as AME and was stored at −80°C as aliquots (0.5–1.0 mL). AME derived from different donors was tested according to the protein concentration determined by BCA assay.

Cell Culturing, Activation by IFN-γ, LPS or IFN-γ/LPS, and AME Treatment

RAW 264.7 cells, a mouse monocyte/macrophage cell line obtained from ATCC, were cultured in phenol red-free DMEM supplemented with 10% FBS, 50 μg/mL gentamicin, and 1.25 μg/mL fungizone. Cells were amplified by passaging once, harvested, and preserved in aliquots in liquid nitrogen. We designated these preserved cells as passage 2 (P2), and used P2 cells for all experiments described here to reduce variation. Cells were seeded in the DMEM/10% FBS medium for cultivation. When they reached 70% to 80% confluence, the cells were treated with trypsin/EDTA for 15 minutes at 37°C. After incubation, cells still firmly attached to the culture dish. Therefore, trypsin/EDTA was removed, 10 mL DMEM/10% FBS was added, and cells were detached by pipetting and collected by centrifugation at 600*g* for 5 minutes. Cell pellets were resuspended in the culture medium, counted, adjusted to the desired density (e.g., 1×10^5/mL), and seeded in a 96-well plate (100 μL/well), a 24-well plate (500 μL/well), or an 8-well chamber slide (250 μL/well). For IFN-γ, LPS, and IFN-γ/LPS stimulation, after cells were seeded for 24 hours, the medium was replaced with the fresh medium containing 200 U/mL IFN-γ, 1 μg/mL LPS, or a combination of both in each well. For AME treatment, an equal volume of PBS (as buffer control) or AME (100 μg/mL total protein, which contained approximately 5 μg/mL hyaluronan) was simultaneously added to the culture medium with IFN-γ, LPS, or IFN-γ/LPS except for those indicated otherwise. At specified time points (e.g., 24 hours), cell cultures were terminated and subjected to MTT assay, and the media and cells were collected/lysed/fixed separately for ELISA, Western blot, or immunocytochemistry/immunofluorescence.

Cell Growth by MTT Assay

After completing stimulation with IFN-γ, LPS, IFN-γ/LPS, or AME treatment, 10 μL MTT reagent was added to each 96-well plate (containing100 μL culture medium). The plate was incubated at 37°C with 5% CO_2 for 4 hours, and 100 μL lysis buffer (containing 10% SDS) was added to each well and incubated for 16 to 20 hours to solublize the crystals. Absorbance was measured at 550 nm and 670 nm (reference wavelength) with the use of an analyzer (Fusion Universal Microplate Analyzer; Packard, Meriden, CT). The subtracted absorbance (550 nm − 670 nm) was correlated with the cell growth/viability.

Cell Death Detection ELISA Assay

Cell lysates equivalent to 10^4 cells after 24-hour stimulation by IFN-γ, LPS, or IFN-γ/LPS with or without AME treatment were collected separately for assay (Cell Death Detection ELISA^{PLUS} Assay; Roche Applied Science) according to the manufacturer's instructions. This ELISA is a photometric enzyme immunoassay for in vitro qualitative and quantitative determination of cytoplasmic histone-associated DNA fragments (mononucleosomes and oligonucleosomes) generated by apoptotic cell death using mouse monoclonal anti-histone and anti-DNA antibodies. Positive and negative controls were included as provided by the manufacturer, and absorbance was measured at 405 nm (Fusion Universal Microplate Analyzer; Packard).

Quantitation of Cell Spreading

Unspread cells were defined as round cells, whereas spread cells were defined as cells with extended pseudopods. The percentage of cells adopting the spread morphology was quantitated by analyzing at least 150 cells from three randomly selected fields, similar to what was reported.[12]

Staining of Actin Filaments with Fluorescein Phalloidin

Cells were fixed in 4% paraformaldehyde/PBS (pH 7.0) for 10 minutes at 25°C. Cells were rinsed three times for 5 minutes each with PBS and then incubated in 0.2% Triton X-100 for 10 minutes. After three rinses with PBS for 5 minutes each and preincubation with 2% BSA to block nonspecific staining, cells were stained with 5 to 10 μm/mL fluorescein phalloidin for 20 minutes. After three additional PBS washes for 5 minutes each, nuclei were stained with Hoechst 33342 (1 μg/mL in PBS) for 15 minutes. Samples were washed three times with PBS, mounted with medium for fluorescence (Vectashield; Vector Laboratories, Inc. Burlingame, CA), and analyzed with a fluorescence microscope (2000E; Nikon, Tokyo, Japan).

Extraction of Triton X-100 Soluble or Resistant Actin Fraction

Extraction was performed according to a previously reported method.[13] Briefly, RAW264.7 cells in 24-well plates were rinsed with cold PBS and then extracted for 10 minutes at 4°C by 105 μL/well of the Triton X-100 extraction buffer (50 mM Tris-HCl, pH 7.5, 150 mM NaCl, 1 mM EDTA, 1.0% Triton X-100, supplemented with 1 mM phenylmethylsul-

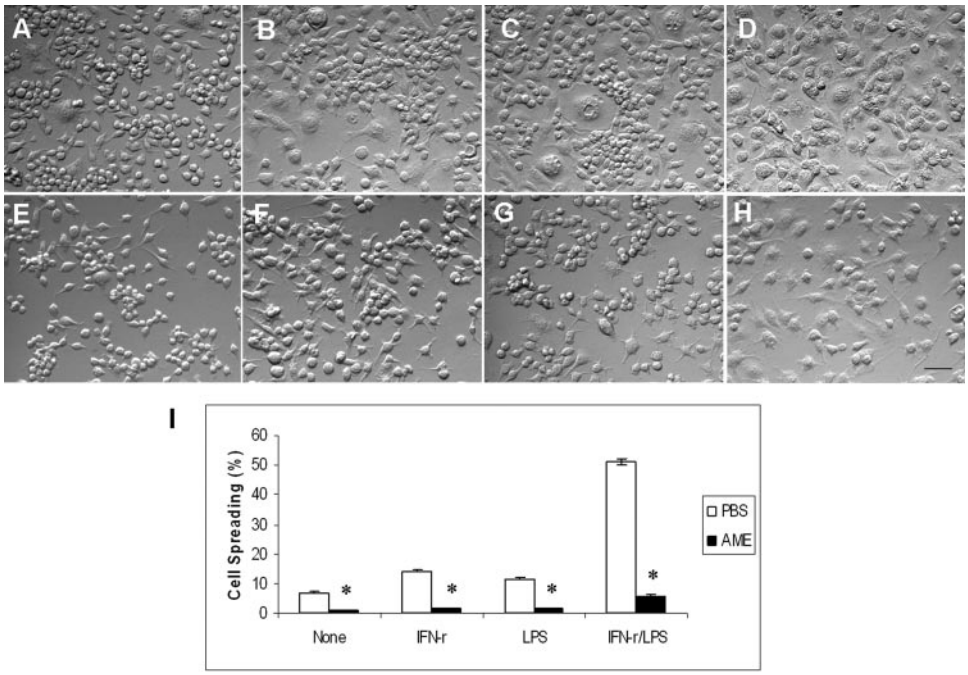

FIGURE 1. Suppression of cell spreading by AME in resting and activated macrophages. Phase-contrast micrographs showed that cell spreading marked by spindle or large squamous cells increased when resting RAW264.7 cells (**A**) were activated by IFN-γ (**B**), LPS (**C**), or LPS/IFN-γ (**D**). In contrast, the number of spindle or large squamous cells was reduced by AME (**E–H**). Scale bar, 50 μm. The percentage of cell spreading was significantly suppressed by AME in resting and activated macrophages (**I**). The result represented mean ± SD ($n = 3$). $^*P < 0.01$.

fonyl fluoride, a cocktail of protease inhibitors, 50 mM sodium fluoride, and 0.2 μM sodium vanadate). The soluble solution (Triton X-100 soluble fraction) was removed. The Triton X-100 insoluble actin fraction remaining in the well was rinsed three times with 1 mL of the same fresh extraction buffer, then lysed in 35 μL Triton X-100 buffer plus 35 μL of 2× Laemmli electrophoresis sample buffer (Triton X-100 resistant fraction). A proportional volume of Triton X-100 soluble and resistant fraction (3:1) was applied for Western blot analysis.

Western Blot

Total proteins (10–20 μg) from each sample were loaded in each well, electrophoresed on a 4% to 15% gradient SDS-PAGE gel, and transferred to a nitrocellulose membrane. The membrane was probed with specific primary antibodies, followed by incubation with appropriate secondary antibody, and was developed with an enhanced chemiluminescence reagent.

Immunocytochemistry

Fixation and permeabilization of cells were the same as described for phalloidin fluorescein staining. Specific antibodies against CD80, (B7.1), CD86 (B7.2), and MHC class 2 antigen were diluted with 2% BSA/PBS according to the manufacturer's recommendation and incubated with cells overnight at 4°C. After washing with PBS, cells were incubated with biotin-conjugated secondary antibodies for 30 minutes, followed by incubation with avidin-peroxidase for 30 minutes. Staining was developed with DAB (1 mg/mL in substrate buffer) for 2 to 10 minutes and was stopped by wash with PBS. Samples were mounted and observed under a contrast microscope (2000E; Nikon).

Immunoassays of Mouse TNF-α, IL-6, and IL-10

Mouse tumor necrosis factor alpha (TNF-α), IL-6, or IL-10 concentrations in cell culture media were determined by solid-phase ELISA (Quantikine/Mouse; R&D Systems) TNF-α immunoassay. Briefly, a monoclonal antibody specific for TNF-α, IL-6, or IL-10 was precoated onto a microplate. Standards and cell culture medium samples (for measuring TNF-α, cell culture medium was diluted 1:5) were pipetted into the wells, and any of these three cytokines was bound by the respective immobilized antibody. After unbound substances were washed away, an enzyme-linked polyclonal antibody specific for TNF-α, IL-6, or IL-10 was added to the wells. After washes to remove any unbound antibody-enzyme reagent, a substrate solution was added to develop color reaction to be measured at 450 nm, with subtraction from that measured at 540 nm. TNF-α, IL-6, or IL-10 concentration in each cell culture medium was then calculated from its respective standard curve.

Statistical Analysis

All experiments were performed at least in triplicate. Summary data were reported as mean ± SD, compiled, and analyzed (MicroSoft Excel; MicroSoft, Redmond, WA). Mean ± SD was calculated for each group using the appropriate version of Student's unpaired *t*-test. Test results were reported as two-tailed *P* values, where $P < 0.05$ was considered statistically significant.

RESULTS

Suppression of Cell Spreading of Resting and Activated Macrophages

We previously reported that AM induced apoptosis of IFN-γ–activated murine monocyte/macrophage RAW264.7 cells in a serum-free culture medium (DMEM/ITS).[11] To examine whether AME still retained similar anti-inflammation activity, we cultivated RAW264.7 cells in DMEM/10% FBS for 24 hours to allow cell adhesion to plastic culture dishes and then incubated them for another 24 hours with fresh medium containing PBS (as the vehicle control) or 100 μg/mL AME (MTT assay; see Fig. 4A for dose predetermination). Under microscopic observation, cells cultivated in PBS adopted three morphologies. Most cells were small and round, some were spindlelike, and some were squamous and dendritic and had pseudopods (Fig. 1A). In contrast, when cells were incubated with AME, cell spreading was markedly reduced, as evidenced by cell adoption of a rounded shape and by reduced numbers of squamous cells (Fig. 1E). Such a morphologic change induced by AME was dose dependent in the range from 0 to 200 μg/mL (not shown here; see Fig. 4A). When activated by 200 μm/mL IFN-γ

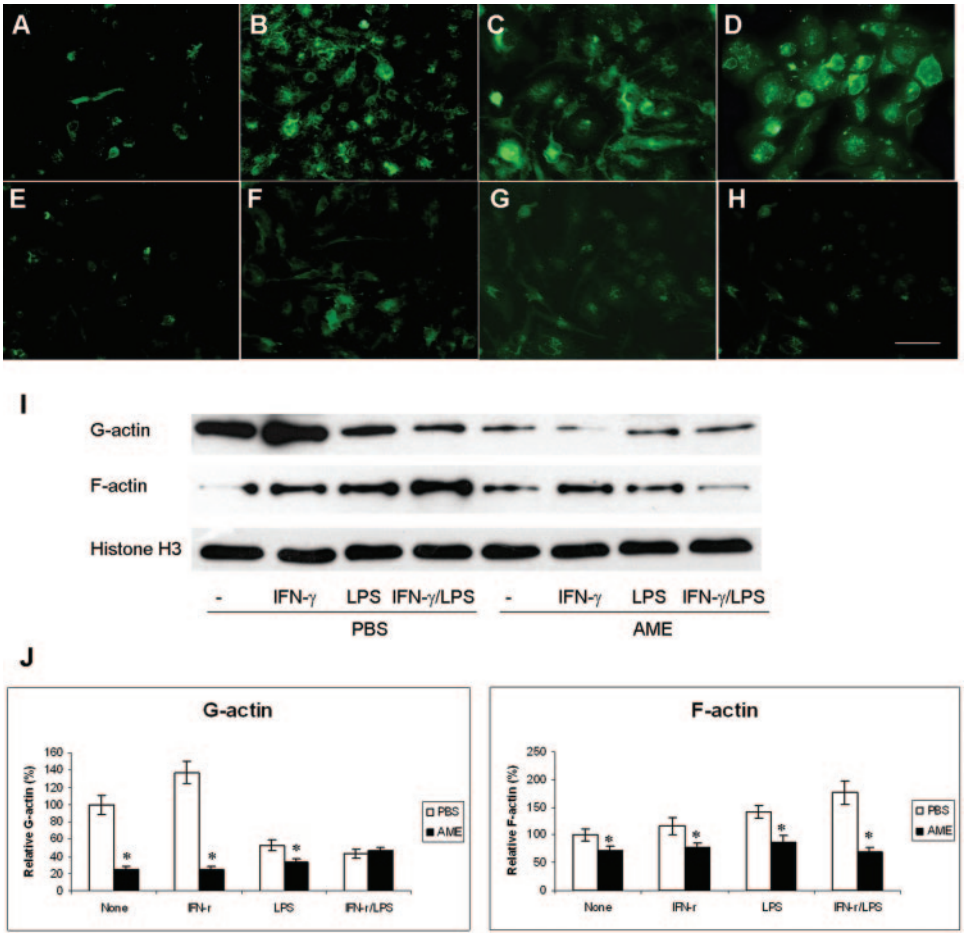

FIGURE 2. Reduction of actin filaments by AME in resting and activated macrophages. Phalloidin staining was weak in resting (**A**) but strong in IFN-γ–activated (**B**), LPS-activated (**C**), and IFN-γ/LPS– activated (**D**) RAW264.7 cells. Such staining was attenuated by 100 μg/mL AME (**E–H**). Scale bar, 50 μm. β-Actin Western blot of Triton X-100 soluble (G-actin) or Triton X-100 resistant (F-actin) cell lysates showed that most total actin was G-actin in resting cells, whereas F-actin increased after activation by IFN-γ, LPS, or both when histone H3 was used as a loading control. In contrast, AME treatment reduced G-actin and F-actin after each activation (**I**, **J**). The result represented mean ± SD ($n = 3$). $^*P < 0.01$.

(Fig. 1B), 1 μg/mL LPS (Fig. 1C), or a combination of both (Figs. 1B–D) for 24 hours, cells became larger and spread further. Under each of these conditions, the simultaneous addition of AME resulted in more rounded cells and fewer squamous cells (Figs. 1F–H, respectively). The percentage of squamous cells, an index reflecting the extent of cell spreading, was significantly increased by IFN-γ, LPS, or IFN-γ/LPS from 6.9 ± 0.15 (resting) to 14.3 ± 0.19, 11.7 ± 0.08, and 50.1 ± 1.03, whereas the addition of AME significantly reduced it to 0.8 ± 0.04, 1.7 ± 0.08, 1.7 ± 0.15, and 5.7 ± 0.62 (Fig. 1I, $P < 0.01$ for all four groups). Such morphologic changes induced by AME could not be elicited by 100 μg/mL BSA or 5 μg/mL hyaluronan (found in 100 μg/mL total protein of AME) (data not shown). These results indicated that AME specifically decreased cell spreading of resting and IFN-γ–, LPS-, and IFN-γ/LPS–activated macrophages.

Reduced Actin Filaments in Macrophages

We speculated that the aforementioned morphologic changes caused by AME regarding cell spreading were mediated by changes in actin filaments because it has been reported that proinflammatory factors such as IFN-γ, LPS, and IFN-γ/LPS can increase actin filaments.[14] To test this hypothesis, we examined actin filaments in RAW264.7 cells by fluorescein-conjugated phalloidin, which binds to the filamentous actin (F-actin) but not the globular actin (G-actin), after cells were stimulated by IFN-γ, LPS, or both in the presence of either PBS or AME for 24 hours (Fig. 2). The results showed that staining to actin filaments was weak and limited around the cell membrane in resting cells (Fig. 2A) but became much stronger and extended to the cytoplasm after activation by IFN-γ, LPS, or IFN-γ/LPS (Figs. 2B–D). In contrast, the addition of AME reduced the intensity of staining to actin filaments in resting and activated macrophages (Figs. 2E–H). To verify this finding, we performed Western blot analysis of Triton X-100 soluble fraction (for G-actin) and Triton X-100 resistant fraction (for F-actin) with histone H3 protein as the loading control (Figs. 2I, 2J). The results showed that approximately 85% of total actin was G-actin in control (PBS) resting cells. LPS and IFN-r/LPS stimulation reduced the G-actin amount considerably—to approximately 68% and 58%, respectively—whereas IFN-γ increased the G-actin amount to approximately 137% compared with that of control resting cells. In contrast, the relative amount of G-actin in AME-treated resting cells was greatly reduced to approximately 25%. LPS or IFN-r/LPS stimulation of AME-treated cells increased the G-actin amount, but IFN-r alone barely changed it. The amount of F-actin was progressively increased by IFN-γ, LPS, or IFN-γ/LPS stimulation to 115%, 140%, or 176%, respectively, that of control resting cells. AME treatment attenuated F-actin in resting and activated cells (from 72% to 77%, 87%, and 90%). Collectively, these data confirmed that AME indeed reduced actin filaments in resting and activated macrophages, explaining the aforementioned morphologic changes and reduced spreading.

Downregulation of Expression of CD80, CD86, and MHC Class 2

CD80, CD86, and MHC class 2 are molecules involved in antigen presentation when macrophages are activated. Previ-

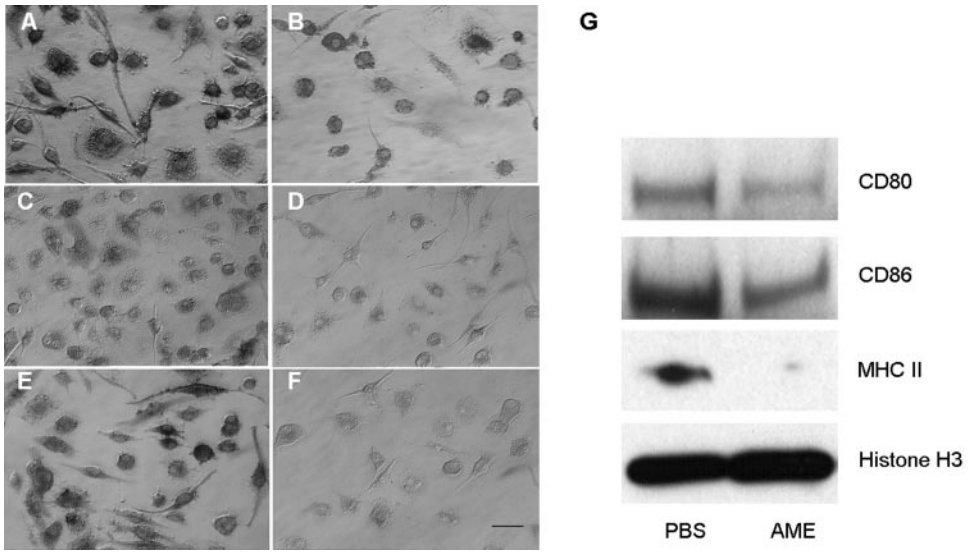

FIGURE 3. Downregulation of CD80, CD86, and MHC class 2 by AME. Expression of CD80 (**A**), CD86 (**C**), and class 2 MHC (**E**) by IFN-γ/LPS–activated RAW264.7 cells was downregulated by AME (**B**, **D**, **F**, respectively). Scale bar, 50 μm. Western blot (**G**) confirmed the downregulation of CD80, CD86, and MHC complex 2 by AME using histone H3 as a loading control.

ous studies have demonstrated that the expression of these cell markers is upregulated in RAW264.7 cells when activated by IFN-γ, LPS, and IFN-γ/LPS.[15,16] We used immunocytochemistry staining to confirm that the expression of CD80, CD86, and class 2 MHC by RAW264.7 cells was upregulated by IFN-γ, LPS (data not shown), or IFN-γ/LPS (Figs. 3A, 3C, 3E). Because AME affected the morphology and reduced the cell spreading and actin filaments of resting and activated RAW264.7 cells, we speculated that the expression of these cell markers was downregulated. As shown in Figures 3B, 3D, and 3F, AME not only decreased the total number of positively stained cells, it reduced the staining intensity in general. For Western blot analysis, we used histone H3 protein as a loading control because the amount of soluble actin (G-actin) in resting and activated cells was affected by AME treatment (Fig. 2). The results confirmed that the level of CD80, CD86, and MHC class 2 proteins was reduced by AME, suggesting that AME further attenuated differentiation of RAW264.7 cells into antigen-presenting cells (APCs) or dendritic cells (DCs) under the stimulation of IFN-γ, LPS, or IFN-γ/LPS.

Suppression of Cell Viability and Enhanced Cell Apoptosis

In vivo, macrophages are produced in large amounts by the bone marrow; most macrophages die shortly after production through apoptosis, depending on the presence or absence of extracellular cues. Some macrophages survive after they are activated by and fully functional through IFN-γ, a cytokine released by activated T lymphocytes and LPS, a component of the cell membranes of Gram-negative bacteria.[17] To determine whether the aforementioned morphologic changes would lead to changes in cellular viability, RAW264.7 cells were cultured in DMEM/10% FBS with or without a series of concentrations of AME. Compared with the control, cellular viability measured by MTT assay was indeed significantly suppressed by AME in a dose-dependent manner after 24 hours of culturing (Fig. 4A). Such inhibition was also observed when cells were simultaneously activated with IFN-γ, LPS, or both (Fig. 4B). We then sought to determine whether AME induced cell death/apoptosis, as AM does in our recent report.[11] Without AME, live/dead assay showed that some cells died under the resting state but that more often cell death was caused by IFN-γ (not shown), LPS (not shown), or IFN-γ/LPS (Figs. 4Ca, 4Cb). However, under either resting or IFN-γ/LPS activation, the addition of AME induced significantly more cell death (Figs. 4Cc, 4Cd). To further determine whether AME induced cell apoptosis, we used a one-step sandwich ELISA (Cell Death Detection ELISA; Roche) method, which specifically quantitates fragmented DNA/histone released into the cytoplasm. The result showed that AME significantly promoted apoptosis in resting and IFN-γ–, LPS-, or IFN-γ/LPS–activated macrophages after 24-hour incubation (Fig. 4D). These results collectively suggested that the above morphologic changes caused by AME also led to the suppression of cell viability and induced cell apoptosis.

Downregulation of TNF-α and IL-6 and Upregulation of IL-10

One mechanism of macrophages regulating the immune response was by releasing proinflammatory cytokines such as tumor necrosis factor (TNF)-α, interleukin (IL)-1, and IL-6. Overproduction of these cytokines, however, was detrimental by prolonging inflammation and aggravating tissue damage. To control the unnecessary inflammation, macrophages also produced negative immunoregulatory cytokines, such as IL-10 and transforming growth factor (TGF)-β, to dampen macrophage activation. To determine whether AME affected the production of proinflammatory and anti-inflammatory cytokines, we used ELISA to measure the concentrations of TNF-α, IL-6, and IL-10 secreted in conditioned media of resting and activated RAW264.7 cells treated with PBS or AME. The amount of TNF-α, IL-6, and IL-10 was further normalized by the total protein present in the each cell lysate extracted by RIPA buffer (50 mM Tris-HCl [pH 7.4], 150 mM NaCl, 1% NP-40, 0.5% deoxycholic acid, 0.1% SDS). Control resting cells secreted a detectable amount of TNF-α (1057 ± 27 pg/mg protein), even without stimulation (Fig. 5A). The induction of TNF-α production by IFN-γ, particularly by LPS or IFN-γ/LPS, was rapid. After 4 hours of stimulation, TNF-α production was significantly increased by IFN-γ–, LPS-, and IFN-γ/LPS–activated macrophages to 2342 ± 270, 16,397 ± 324, and 23,307 ± 216 pg/mg protein, respectively. In comparison, AME significantly reduced TNF-α levels in resting cells (320 ± 81 pg/mg protein; $P = 0.006$) and in IFN-γ, LPS, or IFN-γ/LPS activated cells (1344 ± 135, 11,864 ± 216 and 17,144 ± 351 pg/mg protein; $P = 0.01$, 0.0007 and 0.002, respectively). Compared with TNF-α, IL-6 secreted into the culture medium was lower and slower. After 4 hours of stimulation, IFN-γ /LPS induced barely detectable IL-6 secretion in the culture medium, which was not

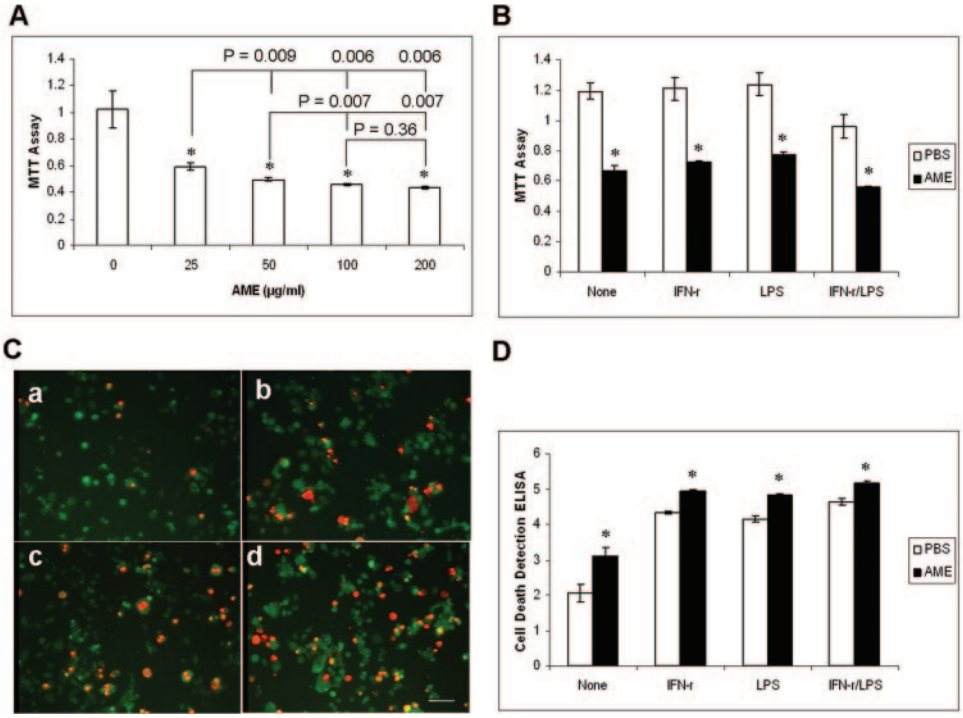

FIGURE 4. Dose-dependent suppression of cell viability of resting and activated macrophages. The cell viability by MTT assay showed dose-dependent suppression by AME in resting RAW264.7 cells (**A**; $n = 4$; $^*P < 0.01$). Such suppression by 100 μg/mL AME was also observed in resting and IFN-γ–, LPS-, and IFN-γ/LPS–activated cells (**B**; $n = 4$; $^*P < 0.01$). Staining with Live/Dead reagent also revealed more dead cells, judged by red fluorescence, when AME was added in resting and IFN-γ/LPS–activated cells (**C** [*upper*], control; [*bottom*], AME; [**a**, **c**], resting; [**b**, **d**], IFN-γ/LPS activated). The extent of cell apoptosis measured by ELISA was also significantly increased by AME in resting and IFN-γ–, LPS-, and IFN-γ/LPS–activated cells (**D**; $n = 4$; $^*P < 0.01$).

significantly different between the control and AME-treated group ($P = 0.06$). After 24 hours of stimulation, IFN-γ produced barely detectable IL-6, a result similar to what has been reported by others.[18,19] In contrast, LPS and IFN-γ/LPS induced significant amounts of IL-6 (Fig. 5B). Under the latter two conditions, AME significantly reduced IL-6 production ($P = 0.04$ and $P = 0.02$, respectively). IL-10 levels were barely detectable after 4 hours of stimulation of IFN-γ, LPS, or IFN-γ/LPS but was significantly increased after 24 hours of stimulation by IFN-γ and more so by LPS and IFN-γ/LPS. AME significantly enhanced IL-10 production under each stimulation by IFN-γ, LPS, and IFN-γ/LPS ($P = 0.05$, $P = 0.04$, and $P = 0.02$, respectively). These data consistently showed that AME downregulated the production of proinflammatory cytokines while it upregulated that of anti-inflammatory cytokines, likely leading to a dampening of macrophage activation and a reduction of inflammation.

DISCUSSION

Previously, we reported that AM stroma induces apoptosis of IFN-γ–activated RAW264.7 cells in vitro by downregulating NF-κB and Akt-FKHR signaling.[11] As a first step toward identifying putative factor(s) in AM responsible for inducing such macrophage apoptosis, we sought to determine whether such an activity was retained in AM-soluble extracts. Herein, we present data showing AME had an effect on macrophages similar to that of AM. AME induced morphologic changes such as cell rounding (Fig. 1), enhanced cell apoptosis (Fig. 4), and

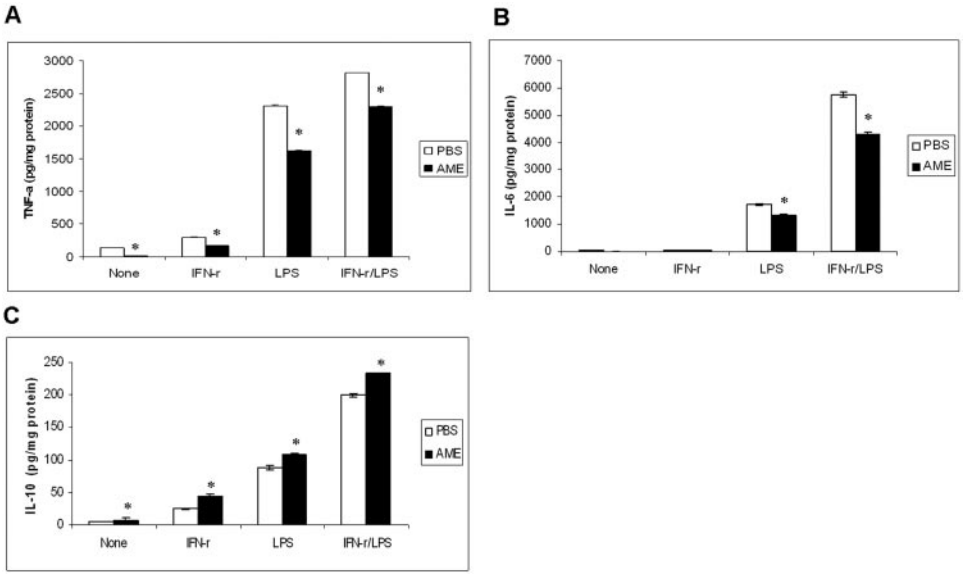

FIGURE 5. Immunoassays of TNF-α, IL-6, and IL-10. With the use of each respective immunoassay, levels of TNF-α (**A**), IL-6 (**B**), and IL-10 (**C**) were measured in conditioned media of resting (none) and IFN-γ, LPS, and IFN-γ/LPS activated RAW264.7 cells in the presence (*black*) or absence (*white*) of AME, and the amount of each cytokine secreted into the cell culture medium was normalized with the total protein in each cell lysate ($n = 4$; $^*P < 0.05$). TNF-α levels were increased more in the order of IFN-γ, LPS, or IFN-γ/LPS activation for 4 hours. IL-6 levels were increased by LPS or IFN-γ/LPS but barely by IFN-γ alone after 24 hours. AME attenuated IL-6 production significantly under these two conditions. In contrast, IL-10 levels were increased by IFN-γ, LPS, or IFN-γ/LPS after 24 hours, and AME significantly enhanced its production in resting and activated macrophages.

downregulated NF-κB signaling while NO synthesis was upregulated (our unpublished data, 2006). Based on these data, we believe the activity of inducing apoptosis of IFN-γ–activated RAW264.7 cells by AM stroma is retained in AME. Given that AME did not cause apoptosis of human corneal fibroblasts whereas heat-treated AME (95°C for 10 minutes) abolished the aforementioned apoptosis of macrophages (not shown), we believe the anti-inflammatory activity of AME is specific to macrophages and may be exerted by their protein component(s). At this stage, we do not know whether such activity is also contributed by amniotic epithelial cells. It is important to point out that certain conditions used in previous and current experiments are different. For example, in our current experiments, macrophages were continuously cultured in DMEM/10% FBS but not in DMEM/ITS and were treated with IFN-γ, LPS, or IFN-γ/LPS after seeding for 24 hours but not for 1 hour. Apoptosis induced by AME was significantly higher when cells were cultured in DMEM/ITS than if they were cultured by DMEM/10% FBS, especially if cells were seeded for a shorter time, which explained why the extent of apoptosis induced by AM stroma was more dramatic than that by AME.

AME dose dependently altered cell morphology by reducing cell spreading (Fig. 1). Such a morphologic change was correlated with a reduction of filamentous actins in resting and activated macrophages (Fig. 2). It is known that reorganization of the actin cytoskeleton is an early cellular response to a variety of extracellular signals, which activate pathways mediated by tyrosine kinase receptors, integrins, G protein–coupled receptors, and Toll-like receptors.[3] The inhibition of RhoA results in disassembly of actin filaments whereas the inhibition of Rac1 and Cdc42 induces cell rounding and loss of cell-substratum adhesion in macrophages.[20] Therefore, further studies on how AME might inhibit the activity of RhoA, Rac1, or Cdc42 may shed more insight into the mechanism regarding this morphologic change.

Facilitation of macrophage apoptosis is desirable to curtail unwanted inflammation. IFN-γ or LPS treatment of macrophages arrests macrophage cell cycle and causes apoptosis,[21,22] though in certain type cells IFN-γ may serve as a survival signal.[23] Consistent with this view, IFN-γ and LPS induced macrophage apoptosis under our experimental conditions; surprisingly, such apoptosis was further enhanced by AME (Figs. 4C, 4D). Our experiments revealed that AME reduced the viability measured by MTT assay by approximately 50%, whereas it increased the apoptosis of activated macrophages by approximately 10% to 15% (Figs. 4B, 4D). MTT assay measures cell viability and cell metabolic activity related to esterase activity; we speculated that AME induced cell death/apoptosis and decreased cell metabolic (esterase) activity without causing cell deaths (at least for the 24-hour period of our experiments). AME also induced apoptosis in resting cells, suggesting that AME might act independently of IFN-γ or LPS. One possible mechanism is to downregulate NF-κB and Akt-FKHR signaling, as previously reported.[11] However, the other plausible mechanism might be through anoikis because AME reduced actin filaments (Fig. 2), caused cell rounding, and slowed cell spreading (Fig. 1). Anoikis is a form of apoptosis induced by cells detaching from the surrounding extracellular matrix.[24] Further experiments are needed to determine whether anoikis is involved in macrophage apoptosis induced by AME.

Morphologic changes were also reflected by the downregulation of cellular activation into antigen-presenting cells, as evidenced by significant reductions in the expression of such cell surface markers as CD80, CD86, and MHC class 2 antigen in resting and activated macrophages (Fig. 3). As a result, we also noted that the levels of secreted proinflammatory cytokines, such as TNF-α and IL-6, were significantly reduced, whereas those of an anti-inflammatory cytokine, such as IL-10, were significantly enhanced (Fig. 5). At this stage we do not know whether an increase of IL-10 is a direct effect by AME because interactions between monocytes/macrophages and apoptotic cells further augment IL-10 production.[25] IL-10 can inhibit monocyte survival and prevent its differentiation into macrophages.[26] Collectively, these data indicated that one putative mechanism for AME to exert its anti-inflammatory action was to downregulate macrophage activation.

References

1. Singer AJ, Clark RA. Cutaneous wound healing. *N Engl J Med*. 1999;341:738–746.
2. Duffield JS. The inflammatory macrophage: a story of Jekyll and Hyde. *Clin Sci (Lond)*. 2003;104:27–38.
3. Lasunskaia EB, Campos MN, de Andrade MR, et al. Mycobacteria directly induce cytoskeletal rearrangements for macrophage spreading and polarization through TLR2-dependent PI3K signaling. *J Leukoc Biol*. 2006;80:1480–1490.
4. Tseng SCG, Tsubota K. In: Holland EJ, Mannis MJ, eds. *Ocular Surface Disease*. 1st ed. New York: Springer. 2002;226–231.
5. Dua HS, Gomes JA, King AJ, et al. The amniotic membrane in ophthalmology. *Surv Ophthalmol*. 2004;49:51–77.
6. Bouchard CS, John T. Amniotic membrane transplantation in the management of severe ocular surface disease: indications and outcomes. *Ocul Surface*. 2004;2:201–211.
7. Heiligenhaus A, Meller D, Meller D, et al. Improvement of HSV-1 necrotizing keratitis with amniotic membrane transplantation. *Invest Ophthalmol Vis Sci*. 2001;42:1969–1974.
8. Park WC, Tseng SCG. Modulation of acute inflammation and keratocyte death by suturing, blood and amniotic membrane in PRK. *Invest Ophthalmol Vis Sci*. 2000;41:2906–2914.
9. Wang MX, Gray TB, Parks WC, et al. Corneal haze and apoptosis is reduced by amniotic membrane matrix in excimer laser photoablation in rabbits. *J Cat Refract Surg*. 2001;27:310–319.
10. Shimmura S, Shimazaki J, Ohashi Y, et al. Antiinflammatory effects of amniotic membrane transplantation in ocular surface disorders. *Cornea*. 2001;20:408–413.
11. Li W, He H, Kawakita T, et al. Amniotic membrane induces apoptosis of interferon-gamma activated macrophages in vitro. *Exp Eye Res*. 2006;82:282–292.
12. Tu Y, Wu S, Shi X, et al. Migfilin and Mig-2 link focal adhesions to filamin and the actin cytoskeleton and function in cell shape modulation. *Cell*. 2003;113:37–47.
13. Cao F, Yanagihara N, Burke JM. Progressive association of a "soluble" glycolytic enzyme with the detergent-insoluble cytoskeleton during in vitro morphogenesis of MDCK epithelial cells. *Cell Motil Cytoskeleton*. 1999;44:133–142.
14. Shinji H, Kaiho S, Nakano T, et al. Reorganization of microfilaments in macrophages after LPS stimulation. *Exp Cell Res*. 1991;193:127–133.
15. Randolph GJ, Beaulieu S, Lebecque S, et al. Differentiation of monocytes into dendritic cells in a model of transendothelial trafficking. *Science*. 1998;282:480–483.
16. Banchereau J, Briere F, Caux C, et al. Immunobiology of dendritic cells. *Annu Rev Immunol*. 2000;18:767–811.
17. Celada A, Nathan C. Macrophage activation revisited. *Immunol Today*. 1994;15:100–102.
18. Kakutani R, Adachi Y, Kajiura H, et al. Relationship between structure and immunostimulating activity of enzymatically synthesized glycogen. *Carbohydr Res*. 2007;342:2371–2379.
19. Ripoll VM, Irvine KM, Ravasi T, et al. Gpnmb is induced in macrophages by IFN-gamma and lipopolysaccharide and acts as a feedback regulator of proinflammatory responses. *J Immunol*. 2007;178:6557–6566.
20. Allen WE, Jones GE, Pollard JW, et al. Rho, Rac and Cdc42 regulate actin organization and cell adhesion in macrophages. *J Cell Sci*. 1997;110(pt 6):707–720.

21. Xaus J, Cardo M, Valledor AF, et al. Interferon gamma induces the expression of p21waf-1 and arrests macrophage cell cycle, preventing induction of apoptosis. *Immunity*. 1999;11:103–113.
22. Xaus J, Comalada M, Valledor AF, et al. LPS induces apoptosis in macrophages mostly through the autocrine production of TNF-alpha. *Blood*. 2000;95:3823–3831.
23. Bernabei P, Coccia EM, Rigamonti L, et al. Interferon-gamma receptor 2 expression as the deciding factor in human T, B, and myeloid cell proliferation or death. *J Leukoc Biol*. 2001;70:950–960.
24. Frisch SM, Screaton RA. Anoikis mechanisms. *Curr Opin Cell Biol*. 2001;13:555–562.
25. Bzowska M, Guzik K, Barczyk K, et al. Increased IL-10 production during spontaneous apoptosis of monocytes. *EurJ Immunol*. 2002;32:2011–2020.
26. Hashimoto SI, Komuro I, Yamada M, et al. IL-10 inhibits granulocyte-macrophage colony-stimulating factor-dependent human monocyte survival at the early stage of the culture and inhibits the generation of macrophages. *J Immunol*. 2001;167:3619–3625.